Available online at www.sciencedirect.com
ScienceDirect
Acta Materialia 58 (2010) 2887–2897
Acta MATERIALIA
www.elsevier.com/locate/actamat

Hafnium binary alloys from experiments and first principles

Ohad Levy [a,b], Gus L.W. Hart [c], Stefano Curtarolo [a,*]

[a] Department of Mechanical Engineering and Materials Science and Department of Physics, Duke University, Durham, NC 27708, USA
[b] Department of Physics, NRCN, P.O. Box 9001, Beer-Sheva, Israel
[c] Department of Physics and Astronomy, Brigham Young University, Provo, UT 84602, USA

Received 28 July 2009; received in revised form 13 January 2010; accepted 17 January 2010
Available online 20 February 2010

Abstract

Despite the increasing importance of hafnium in numerous technological applications, experimental and computational data on its binary alloys is sparse. In particular, data is scant on those binary systems believed to be phase-separating. We performed a comprehensive study of hafnium binary systems with alkali metals, alkaline earths, transition metals and metals, using high-throughput first-principles calculations. These computations predict novel unsuspected compounds in six binary systems previously believed to be phase-separating. They also predict a few unreported compounds in additional systems and indicate that some reported compounds may actually be unstable at low temperatures. We report the results for the following systems: AgHf, AlHf, AuHf, BaHf*, BeHf, BiHf, CaHf*, CdHf, CoHf, CrHf, CuHf, FeHf, GaHf, HfHg, HfIn, HfIr, HfK*, HfLa*, HfLi*, HfMg, HfMn, HfMo,HfNa*, HfNb*, HfNi, HfOs, HfPb, HfPd, HfPt, HfRe, HfRh, HfRu, HfSc, HfSn, HfSr*, HfTa*, HfTc, HfTi, HfTl, HfV*, HfW, HfY*, HfZn and HfZr (* = systems in which the ab initio method predicts that no compounds are stable).

Keywords: Hafnium alloys; High throughput Ab initio calculations

High-throughput (HT) calculations of material properties based on density functional theory (DFT) have been developed in recent years for theoretically guided material discovery and improvement [1–8]. These calculations give insights into trends in alloy properties and indicate possible existence of hitherto unobserved compounds. In this paper we apply the HT approach to a comprehensive screening of hafnium intermetallic binary alloys. This choice is motivated by the wide array of technological applications of hafnium alloys in contrast with their scant theoretical discussion in the literature.

Hafnium is primarily used in the control and safety mechanisms of nuclear reactors, because of its high cross-section for neutron absorption and its high corrosion resistance [9]. Hafnium cladding of nuclear fuel rods is expected to be an important element in the design of future advanced reactors [10]. Hafnium is used extensively as an alloying element in nickel-, niobium- and tantalum-based superalloys, which are designed to withstand high temperatures and pressures. It is an important addition to some titanium, tungsten and molybdenum alloys, where it forms second-phase dispersions (with carbon) that improve material strength under extreme conditions [9,11]. Hafnium alloys are also used in medical implants and devices, due to their biocompatibility and corrosion resistance (see e.g. Ref. [12]). Nickel–titanium–hafnium alloys exhibit shape memory behavior with high martensitic transformation temperatures and good mechanical properties [13]. Hafnium is added to aluminum–magnesium–scandium alloys, widely used in aerospace applications, to increase their strength following high temperature thermomechanical processing [14]. Some intermetallic compounds of Hf and the transition metals Fe, Co, Pd and Pt have been investigated as hydrogen-storage materials because of their capability to form hydrides with high hydrogen to metal ratios at room temperature [15].

Hafnium oxide based compounds have recently found wide application replacing silicon oxide as high-k dielec-

* Corresponding author. Tel.: +1 919 660 5506.
E-mail address: stefano@duke.edu (S. Curtarolo).

1359-6454/$36.00 © 2010 Acta Materialia Inc. Published by Elsevier Ltd. All rights reserved.
doi:10.1016/j.actamat.2010.01.017

trics in the production of integrated circuits [16]. This has motivated a few first-principles studies of the dielectric properties of hafnium silicates (see e.g. Ref. [17]). Perovskite alkaline metal hafnates (e.g. $CaHfO_3$, $BaHfO_3$ and $SrHfO_3$) have been investigated for various optical and electronic applications as well as substrates for perovskite superconductor films, due to their high stability in the fabrication process of such films and their small crystallographic mismatch (see e.g. Ref. [18]). Although zirconium has been tried as a cheaper substitute for hafnium, in most of these applications only hafnium produces the desired properties [9].

Despite this wealth of existing and potential applications, computational studies of hafnium compounds are few. In most of these studies, just a few specific structures have been investigated [19–34]. A large number of structures have been examined in only three cases: Al–Hf, Cu–Hf and Hf–Nb [25,35–37]. In the Al–Hf system, the energies of 22 intermetallic structures have been calculated, four of which are ground states and constitute the convex hull of the system [36,37]. The convex hull connects all of the ground states on a concentration vs. enthalpy diagram. The enthalpies of all other structures lie above the tie-lines between the ground states. Thermodynamically, the convex hull represents the Gibbs free energy of the alloy at zero temperature [1,2]. In the Cu–Hf system, energies of 28 structures have been calculated and four identified as ground states [35]. In both cases, differences have been found between the phase diagrams based on calorimetric measurements and the calculated ground states. In contrast, positive formation enthalpies were calculated for 13 Hf–Nb intermetallic structures [25], in agreement with experimental observations that the system is phase-separating.

In several systems, the stability of a few competing structures have been examined, but the complete convex hull of the intermetallic system has not been addressed. These include the ground state properties of five different structures of Hf_3Mo, HfMo and $HfMo_3$ [27] and the three Laves phases of $HfCr_2$ [24], $HfFe_2$ [20,33], HfV_2 [31,33] and $HfMn_2$ [23]. Single specific structures of Hf_2Fe [19,29], Hf_2Co [21], HfB_2 [26,32,34], Hf_2Ni [28], $HfTe_5$ [30], HfRu, HfRh, HfIr and HfPt [22] have also been studied. Some of these compounds were studied because they are used in hyperfine field measurements by the time-dependent perturbed angular correlation (TDPAC) technique, for which ^{183}Hf is an excellent probe, that can be easily compared to first-principles calculations of the local electric field gradient in the vicinity of the probe.

In this paper we report a comprehensive computational study of the low temperature stability of 44 hafnium binary systems; hafnium combined with alkali metals, the alkaline earths, transition metals and metals. We apply the ab initio formation energy criterion, which has been shown to be reliable for binary systems [1,2,41]. The calculations were performed using the high-throughput framework AFLOW [1,42,43], employing ab initio calculations of the energies with the VASP software [44]. We used projector-augmented waves (PAW) pseudo-potentials [45] and the exchange–correlation functionals parameterized by Perdew et al. [46] for the generalized gradient approximation (GGA). The energies were calculated at zero temperature and pressure, with spin polarization, and without zero-point motion or lattice vibrations. All crystal structures were fully relaxed (cell volume and shape and the basis atom coordinates inside the cell). Numerical convergence to about 1 meV $atom^{-1}$ was ensured by a high energy cutoff (40% higher than the highest energy cutoff for the pseudo-potentials of the components) and dense 6000 k-point Monkhorst–Pack meshes. For each system, we calculated the energies of all the ground state structures reported in Refs. [40,39], and about 200 additional crystal structures. In addition to the 176 structures described in Ref. [1], these included the prototypes A5, A6, A7, A11, B20, TlI, ThIn, LiB-MS1/2 [47,48], Au_4Zr, Ca_7Ge, $NbNi_8$ (Pt_8Ti), Ga_2Hf, W_5Si_3, V_4Zn_5, Ni_7Zr_2, C36 and the complete set of hexagonal close-packed (hcp) superstructures [38] with up to four atoms per cell.

Some of our results deviate from the experimental data [39,40]. Table 1 is a summary of the alloy systems addressed in this study. In the first column, the alloying metals are ordered according to their Mendeleev number (or Pettifor's chemical scale) [49,50]. The reported experimental compounds (or lack thereof) are shown in the second column and the calculated ones in the third column. The compounds are presented with their structure *Strukturbericht* designation or prototype in parentheses (unspecified or unknown structures are denoted as Unk.). Some of the predicted phases (marked by an asterisk) have structures for which no prototype is known and no *Strukturbericht* designation have been given. These new prototypes are described in Table 2. Appearance of two structures in the third column indicates their degeneracy. The fourth column gives the calculated energies of the structures identified on the convex hull of each binary system (3rd column). Energies of reported structures (2nd column) that are found to lie above the convex hull (missing in the 3rd column) are indicated in parentheses. In cases where the reported and calculated structures of a compound are different, or two non-degenerate structures are reported, the energy difference between them is indicated in square parentheses. The calculated convex hulls of all the compound-forming systems are shown in Figs. 1–3.

In Table 1 there are 16 systems that are reported in the literature as phase-separating, i.e. having no compounds. Thirteen of these systems are grouped together at the top of the table. It is not surprising to see this same behavior in a block of the table, because the systems are listed by Pettifor's Mendeleev number [50]. The other three systems reported to be phase-separating, Hf–Mg, Hf–Tl and Hf–Pb, are scattered in the lower rows of the table. In these three cases, our calculations show that they are in fact compound-forming, essentially complementing the general trend implied by the Pettifor chemical scale. Stable structures are also found in the binary systems of Hf with Ti and Zr (sharing the IVB column of the periodic table) and Sc. In five of the six systems

Table 1
Compounds observed in experiments or predicted by ab initio calculations in metallic binary alloys of Hf. The structure *Strukturbericht* designation or prototype is given in parentheses (Unk. denotes unknown structures). New prototypes are marked by ★ and described in Table 2. More than one structure may have been reported (2nd column) or found with degenerate energies (3rd column). ΔH are the formation enthalpies of the compounds in the present study; parentheses denote reported structures (2nd column) that lie above the convex hull (missing in the 3rd column). Square parentheses denote energy differences between experimentally observed and calculated structures or two reported non-degenerate structures.

	Compounds		ΔH (meV atom^{-1})
	Experiments [39,40]	Calculations	
K, Na	–	–	
Li, Ba	–	–	
Sr, Ca, Y	–	–	
Sc	–	Hf_5Sc★	−10
		Hf_3Sc★	−10
La	–	–	
Zr	–	$HfZr_2$(C32)	−22
Ti	–	$HfTi_2$(C32)	−11
Nb, Ta	–	–	
V	HfV_2(C15)	–	(31)
Mo	$HfMo_2$(C15)	$HfMo_2$(C15)	−170
W	HfW_2(C15)	HfW_2(C15)	−171
Cr	$HfCr_2$(C15,C36)	$HfCr_2$(C15)	−120[+6]
Tc		$Hf_3Tc(Mo_3Ti$★ [1])	−269
		Hf_2Tc(C49)	−357
	HfTc(B2)	HfTc(B2)	−482
	$HfTc_2$(C14)	$HfTc_2$(C14)	−362
Re		$Hf_3Re(Mo_3Ti$★ [1])	−200
	HfRe (Unk.) [39]		
	$Hf_{21}Re_{25}(Re_{25}Zr_{21})$ [40]	$Hf_{21}Re_{25}(Re_{25}Zr_{21})$	−407
	$HfRe_2$(C14)	$HfRe_2$(C14)	−394
	$Hf_5Re_{24}(Ti_5Re_{24})$	$Hf_5Re_{24}(Ti_5Re_{24})$	−252
Mn	$HfMn_2$(C14, C36)	$HfMn_2$(C14)	−268[+4]
	$Hf_2Mn(NiTi_2)$		(−109)
Fe		$Fe_5Hf(C15_b)$	−178
	Fe_2Hf(C14, C15)	Fe_2Hf(C15)	−354[+14]
		FeHf(B2)	−331
	$FeHf_2(NiTi_2)$		(−189)
Os	$Hf_{54}Os_{17}(Hf_{54}Os_{17})$		(−319)
	$Hf_2Os(NiTi_2)$		(−429)
	HfOs(B2)	HfOs(B2)	−707
	$HfOs_2$(C14)		(−402)
Ru	HfRu(B2)	HfRu(B2)	−819
	$HfRu_2$ (Unk.)		
Co	$Co_7Hf_2(Ni_7Zr_2)$		(−219)
	Co_2Hf(C15)	Co_2Hf(C14)	−374[+3]
	CoHf(B2)	CoHf(B33)	−401[+12]
	$CoHf_2(NiTi_2)$	$CoHf_2$(C37)	−314[+23]
Ir	$Hf_2Ir(NiTi_2)$	Hf_2Ir(C37)	−750[+31]
	$Hf_5Ir_3(D8_8$ [40], Ir_5Zr_3 [39])	$Hf_5Ir_3(Ir_5Zr_3)$	−814[+14]
	HfIr (Unk.)	HfIr(B27)	−949
		$HfIr_2(Ga_2Hf)$	−872
	$HfIr_3(L1_2)$	$HfIr_3(L1_2)$	−800
Rh	$Hf_2Rh(NiTi_2)$	$Hf_2Rh(CuZr_2)$	−632[+12]
	HfRh(B2)	HfRh(B27)	−899[+30]
	$Hf_3Rh_5(Ge_3Rh_5)$	$Hf_3Rh_5(Ge_3Rh_5)$	−928
	$HfRh_3(L1_2)$	$HfRh_3(L1_2)$	−762
Ni	Hf_2Ni(C16)		(−345)
	HfNi(CrB [40], TlI [39])	HfNi(TlI)	−542[+20]
	$Hf_9Ni_{11}(Zr_9Pt_{11})$		(−461)
	$Hf_7Ni_{10}(Zr_7Ni_{10})$		(−520)
	$HfNi_3(BaPb_3)$	$HfNi_3(D0_{24})$	−545[+4]

(*continued on next page*)

Table 1 (*continued*)

	Compounds		ΔH (meV atom^{-1})
	Experiments [39,40]	Calculations	
	$Hf_2Ni_7(Ni_7Zr_2)$		(−470)
	$HfNi_5(C15_b)$		(−350)
Pt	$Hf_2Pt(NiTi_2)$	$Hf_2Pt(NiTi_2)$	−786
	HfPt(B2, B33 [40], TlI [39])	HfPt(B33, TlI)	−1153[+165]
	$HfPt_3(L1_2, D0_{24})$	$HfPt_3(D0_{24})$	−1100[+3]
		$HfPt_8(Pt_8Ti)$	−528
Pd	$Hf_2Pd(C11_b$ [40], $CuZr_2$ [39])	$Hf_2Pd(C11_b, CuZr_2)$	−527
	HfPd (Unk.)	HfPd(B33)	−682
	Hf_3Pd_4 (Unk.)		
	$HfPd_2(C11_b)$	$HfPd_2(C11_b)$	−817
	$HfPd_3(D0_{24}, L1_2)$	$HfPd_3(D0_{24})$	−879[+11]
		$HfPd_5(HfPd_5^{\star})$	−635
		$HfPd_8(Pt_8Ti)$	−430
Au	Au_5Hf [40], $Au_{4.2}Hf_{4.8}$ [39]($D1_a$)		(−407)
	$Au_4Hf(Au_4Zr, D1_a)$	$Au_4Hf(Au_4Zr)$	−414
	$Au_3Hf(D0_a)$	$Au_3Hf(D0_a)$	−483
	$Au_2Hf(C11_b)$	$Au_2Hf(C11_b)$	−565
		$Au_4Hf_3(Cu_4Ti_3)$	−563
	$Au_{10}Hf_7$ (Unk.)		
	AuHf(B11)	AuHf(B11)	−545
	$AuHf_2(C11_b$ [40], $CuZr_2$ [39])	$AuHf_2(C11_b, CuZr_2)$	−440
Ag	AgHf(B11)	AgHf(B11)	−119
	$AgHf_2(C11_b$ [40], $CuZr_2$ [39])	$AgHf_2(C11_b, CuZr_2)$	−122
Cu		$Cu_5Hf(C15_b)$	−129
	$Cu_{51}Hf_{14}(Ag_{51}Gd_{14})$		(139)
	$Cu_8Hf_3(Cu_8Hf_3)$	$Cu_8Hf_3(Cu_8Hf_3)$	−173
	$Cu_{10}Hf_7(Ni_{10}Zr_7)$	$Cu_{10}Hf_7(Ni_{10}Zr_7)$	−186
	$CuHf_2(C11_b$ [40],$CuZr_2$ [39])	$CuHf_2(C11_b, CuZr_2)$	−166
Mg	–	HfMg(CdTi)	−7
Hg	$Hf_2Hg(C11_b$ [40], $CuZr_2$ [39])	$Hf_2Hg(C11_b, CuZr_2)$	−120
Cd	CdHf(B11 [40], CdTi [39])	CdHf(CdTi, B11)	−88
	$CdHf_2(C11_b$ [40], $CuZr_2$ [39])	$CdHf_2(\beta 1)$	−87[+18]
Zn	$Hf_2Zn(C11_b$ [40], $CuZr_2$ [39])	$Hf_2Zn(C11_b, CuZr_2)$	−175
	$HfZn_2$(C36 [40], C15 [39])	$HfZn_2(CaIn_2)$	−233[+18]
	$HfZn_3$ (Unk.)	$HfZn_3(YCd_3)$	−204
	$HfZn_5$ (Unk.)		
	$HfZn_{22}(Zn_{22}Zr)$	$HfZn_{22}(Zn_{22}Zr)$	−43
Be	$Be_{13}Hf(D2_3)$	$Be_{13}Hf(D2_3)$	−173
	$Be_{17}Hf_2(Th_2Ni_{17}, Th_2Zn_{17})$	$Be_{17}Hf_2(Th_2Zn_{17})$	−223[+485]
	$Be_5Hf(D2_d)$	$Be_5Hf(D2_d)$	−226
	Be_2Hf(C32)		(−166)
	BeHf(TlI)		(−75)
Tl	–	$Hf_2Tl(Hf_2Tl^{\star})$	−2
In		$Hf_3In(L1_2)$	−148
	$HfIn(L1_0)$		(−160)
	$Hf_3In_4(In_4Ti_3)$	$Hf_3In_4(In_4Ti_3)$	−285
Al	$Al_3Hf(D0_{22}$ [40], $D0_{23}$ [39])	$Al_3Hf(D0_{23})$	−401[+9]
	Al_2Hf(C14)	Al_2Hf(C14)	−455
	$Al_3Hf_2(Al_3Zr_2)$		(−434)
	AlHf(B33 [40], TlI [39])		(−410)
	$Al_3Hf_4(Al_3Zr_4)$	$Al_3Hf_4(Al_3Zr_4)$	−399
	$Al_2Hf_3(Al_2Zr_3)$		(−338)
	$Al_3Hf_5(D8_8)$		(−299)
	$AlHf_2$(C16)		(−272)
	$AlHf_3$ (Unk.) [39]	$AlHf_3(L1_2)$	−239
Ga	$Ga_3Hf(D0_{22})$		(−382)
	$Ga_2Hf(Ga_2Hf)$		(−456)

Table 1 (*continued*)

	Compounds		ΔH (meV atom^{-1})
	Experiments [39,40]	Calculations	
	$Ga_3Hf_2(Al_3Zr_2)$	$Ga_3Hf_2(Al_3Zr_2)$	−664
	GaHf(InTh)		(−519)
	$Ga_{10}Hf_{11}(Ge_{10}Ho_{11})$		(−495)
	$Ga_3Hf_5(D8_8)$	$Ga_3Hf_5(D8_8)$	−445
	$GaHf_2$(C16)	$GaHf_2$(C16)	−404
Pb	–	$Hf_5Pb^{\star}$	−140
		$Hf_5Pb_3(W_5Si_3)$	−253
Sn	$Hf_5Sn_3(D8_8)$	$Hf_5Sn_3(D8_8)$	−380
	$Hf_5Sn_4(Ga_4Ti_5)$	$Hf_5Sn_4(Ga_4Ti_5)$	−396
	HfSn(B20)		(−270)
	$HfSn_2$(C40)	$HfSn_2$(C40)	−265
Bi	$Bi_2Hf(As_2Ti)$	Bi_2Hf(C16)	−147[+14]
	$Bi_9Hf_8(V_{7.46}Sb_9)$		(−166)
	BiHf (Unk.)	BiHf(B20)	−183
		$BiHf_2^{\star}$	−169

predicted to be compound-forming (excluding Hf–Pb) the pure elements have a hcp crystal structure and only disordered hcp solid solutions have been reported for their binary alloys with hafnium over the entire range of concentrations. The calculations indicate, however, that in four of them stable compounds that are not hcp-based superstructures should exist at low temperatures. Only in the Hf–Sc system are the new compounds predicted to have a hcp-based structure. Three of these metals have very high melting temperatures and the available experimental data on their alloys is also limited to high temperatures above 700 °C, 800 °C, 1000 °C for Ti, Zr and Sc, respectively [39,40]. No data are available for Hf–Mg, Hf–Tl and Hf–Pb alloys.

Following these findings, we carried out a more extensive HT search for additional stable structures in these six binary systems. This search included 137 face-centered cubic (fcc) structures with up to six atoms per cell, 137 body-centered cubic (bcc) structures with up to six atoms per cell and 333 hcp structures with up to eight atoms per cell (enumerated in Ref. [38]). This search found lower energy structures in the Hf–Sc system but failed to improve on the findings of the smaller set search in the other five systems. This demonstrates the efficiency and reliability of the HT approach in finding phase-stability in binary systems using a search base of about 200 structures per system. More extensive searches, on larger sets of derivative structures, seem to be useful only in cases where both elements and their compounds share a common parent lattice.

In contrast to the preceding examples, our calculations predict phase-separation in the Hf–V system, for which the compound HfV_2 has been reported at high temperatures (1000–1550 °C) [39,40]. Calculations of possible structures of this compound show that the lowest energies, all positive, are obtained for C14, C36 and C15 in that order, whereas the structure reported in the literature is C15 [39]. This is in agreement with the calculation in Ref. [31], which also found C14 as the lowest energy structure of these three Laves phases for HfV_2. The compound HfV_2 reported in the literature is therefore unstable at low temperatures. The discrepancy between the computational result of C14 as the minimum energy structure (Hf atoms on the sites of a hexagonal diamond structure) and the observed high temperature C15 phase (Hf on the sites of a diamond structure) may be due to vibrational stabilization at high temperature. In fact, C15 is only 24 meV atom^{-1} above C14 and, given that entropic differences between structures can be of the order of $0.1–1.0\,k_B$ per atom [51], very small energy differences between the experimentally observed structure and our ab initio results could be reversed at elevated temperature. This phenomenon is common; for example, in Ref. [52] the vibrational entropy difference is shown to stabilize the $\theta - Al_2Cu$ (C16) phase over the competing $Al_2Cu - \theta'$ phase (distortion of $\theta_c - C1$), which has the lowest energy and is therefore stable at low temperatures.

In agreement with experimental data, all the other transition metals, from columns VIB to IIB of the periodic table, have stable compounds with hafnium at low temperatures. The situation is especially simple for the VIB metals, chromium, molybdenum and tungsten, for which the calculations confirm the existence of a single compound HfM_2 with a C15 structure. Other Hf–Mo compounds for which ab initio calculations have been previously performed [27] are shown to be unstable. The Hf–Hg system also exhibits a single compound, Hf_2Hg, where the calculations confirm that the reported structures $C11_b$ [40] and $CuZr_2$ [39] are degenerate.

The calculations for the Fe–Hf system show the existence of a stable compound Fe_2Hf with a C15 structure, and the C14 structure just slightly less stable (14 meV atom^{-1}). This is consistent with the literature, where the two structures have been reported [39] at temperatures above 600 °C. However, in contrast to the available experimental data, the calculation shows that the compounds FeHf (B2 structure) and $Fe_5Hf(C15_b)$ are also stable whereas the $FeHf_2$ compound, reported with a $NiTi_2$ structure, is unstable at low

Table 2
Geometry of new prototypes in our study. Positions are given as relaxed positions. $Hf_2Tl^\star$ is a tetragonal distorsion of β_2 [1].

System	$Hf_3Sc^\star$	$Hf_5Sc^\star$	$BiHf_2^\star$
Lattice	Orthorhombic	Hexagonal	Monoclinic
Space Group	Cmcm #63	$P\bar{6}2m$ #189	C2/m #12
Pearson symbol	oS16	hP6	mS12
Prim. vect.	(SG option 2)	(SG option 2)	(SG option 2)
a, b, c (Å)	6.439, 11.153, 5.0372	5.565, 5.565, 5.046	10.974, 3.849, 7.39
α, β, γ (deg)	90, 90, 90	90, 90, 120	90, 66.044, 90
Wyckoff positions	Hf1 0,0.0821,1/4 (4c) Hf2 −0.2546,0.3332,1/4 (8g) Sc1 0,−0.4160,3/4 (4c)	Hf1 −0.3392,0,0 (3f) Hf2 1/3,2/3,1/2 (2d) Sc 0,0,1/2 (1b)	Bi1−0.16985,0,0.13317 (4i) Bi2 0.48100,0,−0.22778 (4i) Hf1 0.14974,0,0.44872 (4i)
AFLOW label [42]	"471"	"473"	"475"
System	$Hf_2Tl^\star$	$Hf_5Pb^\star$	$HfPd_5^\star$
Lattice	Tetragonal	Tetragonal	Orthorhombic
Space Group	I4/mmm #139	P4/mmm #123	Cmmm #65
Pearson symbol	tI6	tP6	oS12
Prim. vect.	(SG option 2)		
a, b, c (Å)	4.422, 4.422, 7.385	3.203, 3.203, 13.944	11.998, 4.0663, 14.0723
α, β, γ (deg)	90, 72.577, 90	90, 90, 90	90, 90, 90
Wyckoff positions	Hf1 0,0,0.1746 (4e) Tl2 0,0,1/2 (2b)	Hf1 0,0,−0.1794 (2g) Hf2 1/2,1/2,−0.3349 (2h) Hf3 0,0,1/2 (1b) Pb1 1/2,1/2,0 (1c)	Hf1 0,0,0 (2a) Pd1 0.1663,0,1/2 (4h) Pd2 0.3369,0,0 (4g) Pd3 1/2,0,1/2 (2c)
AFLOW label [42]	"547"	"477"	"479"

temperatures. Its formation energy is 35 meV atom^{-1} higher than the tie line FeHf(B2) ↔ Hf(A3) and thus could decompose at temperatures lower than 100 °C (Fig. 1). A similar behavior is found in the HfMn system, where the C14 structure of $HfMn_2$ is found to be stable, with the C36 and C15 structures at slightly higher energies (4 and 5 meV atom^{-1}, respectively). The experimentally reported Hf_2Mn compound ($NiTi_2$ prototype) is again found to be unstable at low temperatures, at 30 meV atom^{-1} above the Hf(A3) ↔ $HfMn_2$(C14) tie line.

In the Hf–Ru and Hf–Os systems, a stable B2 structure of HfRu and HfOs is found in agreement with the experiments [39]. The compounds Hf_2Os, $Hf_{54}Os_{17}$ and $HfOs_2$ reported from experimental data are found to be unstable. No stable structure was found for the $HfRu_2$ compound, whose existence was suspected in some experiments [39]. In the Hf–Re system, Ref. [39] reports a $Hf_{21}Re_{25}$ compound (prototype $Re_{25}Zr_{21}$) whereas Ref. [40] reports a HfRe compound of unspecified prototype. Our calculations confirm the existence of the $Hf_{21}Re_{25}$ compound but find no stable structure for HfRh. The lowest HfRh structure, B2, lies approximately 50 meV atom^{-1} above the convex hull (Table 1 and Fig. 2). For the Co–Hf system, our calculations confirm the existence of the stable compounds Co_2Hf, CoHf and $CoHf_2$ at low temperatures, albeit with structures different from those reported in experiments. The reported Ni_7Zr_2 structure of Co_7Hf_2 lies above the convex hull (Table 1 and Fig. 1).

The Cu–Hf system is the only transition metal–hafnium system previously studied by ab initio methods, also using the VASP software but with different potentials than in our study (Vanderbilt-type ultrasoft pseudo-potentials) [35]. Twenty-eight different compound structures have been calculated, of which four, Cu_5Hf, Cu_8Hf_3, $Cu_{10}Hf_7$ and $CuHf_2$, were identified as stable. Our calculations also indicate that these four compounds are stable. There is no experimental information about the structure of Cu_5Hf [39]. We obtain the $AuBe_5$ structure in agreement with Ref. [35]. The $CuZr_2$ structure, reported in experiments for $CuHf_2$ [39] but not calculated in Ref. [35], is degenerate with the reported $C11_b$ structure. The ground state convex hull is asymmetric and skewed towards the Cu side, in agreement with the general conclusions of Ref. [35] (Fig. 1). The Al–Hf system was studied using the same methodology [36]. The convex hull in this case is defined by four compounds, $Al_3Hf(D0_{23})$, $Al_2Hf(C14)$, $Al_3Hf_4(Al_3Zr_4)$ and $AlHf_3(L1_2)$, with $Al_3Hf_2(Al_3Zr_2)$ and AlHf(B33) slightly above the convex hull. Our calculations reproduce these results and show in addition that the AlHf structure TlI, reported in the experimental data but not studied in Ref. [36], is degenerate with B33. Other compounds reported for this system [39] are found to be significantly above the convex hull and should therefore be unstable at low temperatures (see Table 1 and Fig. 1).

Our HT study uncovers a few compounds on which no data are available in the experimental literature [39,40] in the binary systems of Hf with Au, Bi, In, Pd, Pt, Re and Tc. A few reported compounds are found to lie above the convex hull of their respective systems (Hf with Be, Ga, Ni and Sn) and are thus predicted to be unstable at low temperatures (Table 1).

In most cases where two structures are reported in the experimental literature the calculations show that they are indeed degenerate or the energy differences are small,

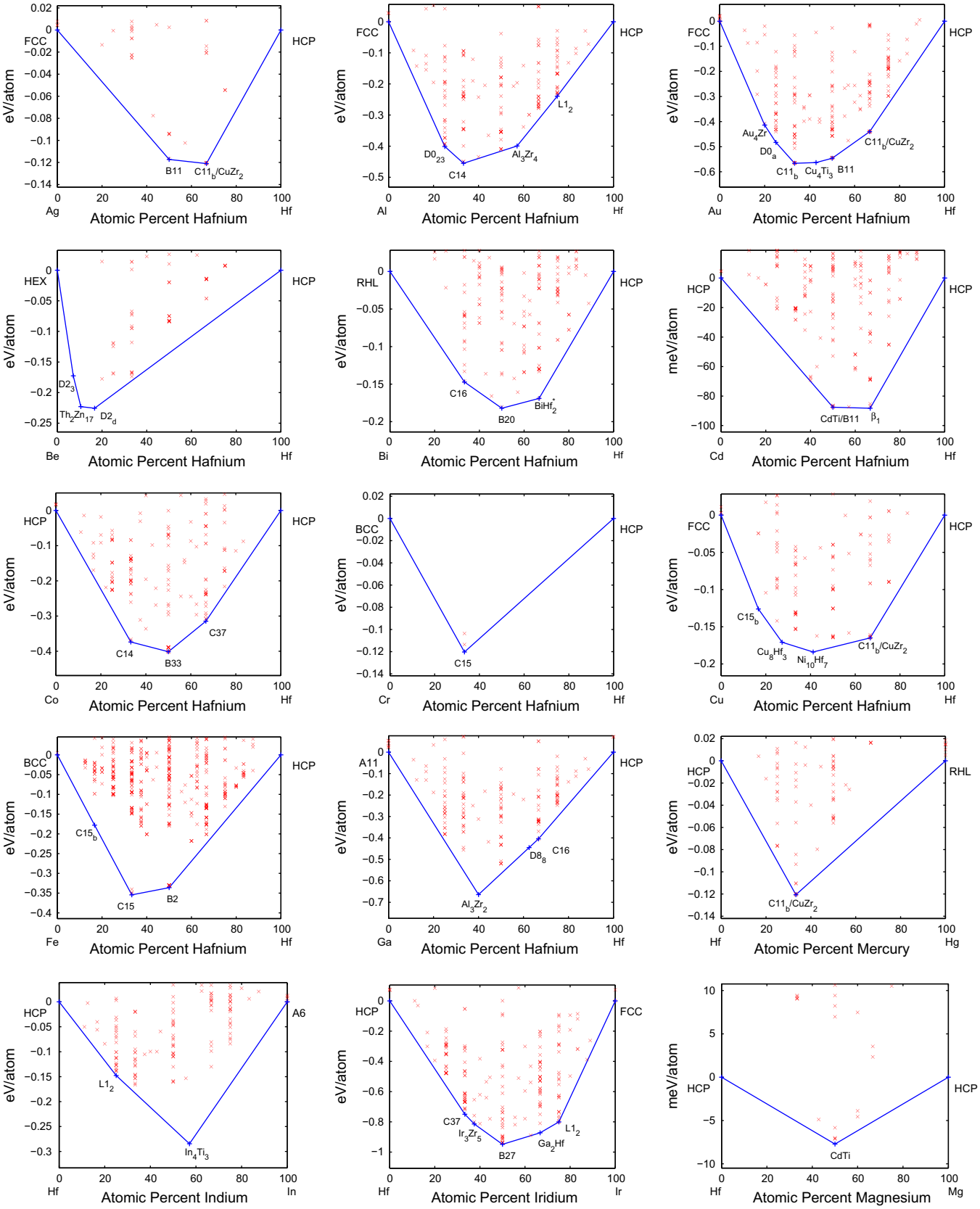

Fig. 1. Formation enthalpies of Ag–Hf, Al–Hf, Au–Hf, Be–Hf, Bi–Hf, Cd–Hf, Co–Hf, Au–Hf, Cu–Hf, Fe–Hf, Ga–Hf, Hf–Hg, Hf–In, Hf–Ir and Hf–Mg alloys.

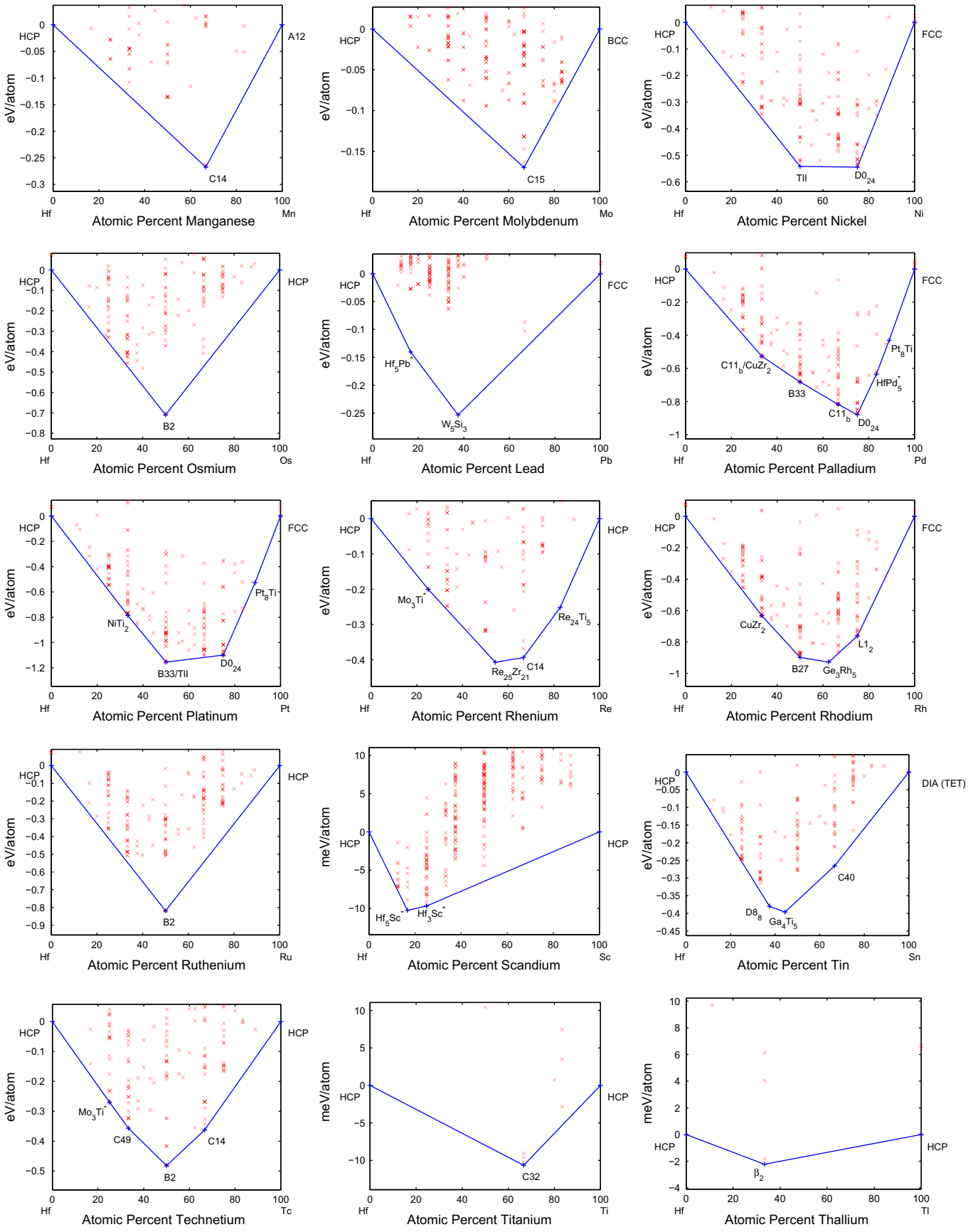

Fig. 2. Formation enthalpies of Hf–Mn, Hf–Mo, Hf–Ni, Hf–Os, Hf–Pb, Hf–Pd, Hf–Pt, Hf–Re, Hf–Rh, Hf–Ru, Hf–Sc, Hf–Sn, Hf–Tc, Hf–Ti and Hf–Tl alloys.

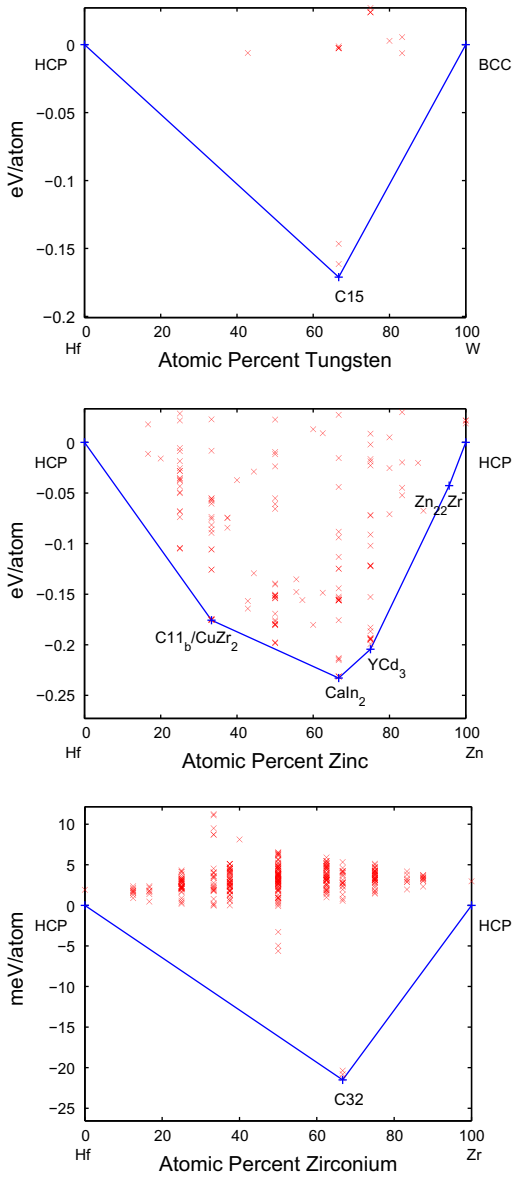

Fig. 3. Formation enthalpies of Hf–W, Hf–Zn and Hf–Zr alloys.

30 meV atom^{-1} or less (square parentheses in Table 1). In only two cases do these structures differ considerably. The B2 structure of HfPt is 165 meV atom^{-1} higher than the degenerate B33/TlI groundstate. No phase diagram is available for the Hf–Pt system, but the experimental data indicate that the B2 structure might have been observed in a non-stoichiometric mixture [40]. The calculations seem to provide an indirect confirmation of this observation, showing that B2 is not a stable structure of the stoichiometric mixture. The Th_2Ni_{17} structure of $Be_{17}Hf_2$ is 485 meV atom^{-1} higher than the Th_2Zn_{17} groundstate (sometimes also denoted as $Be_{17}Nb_2$ [39,40]). As discussed in Ref. [40], it has not been determined whether $Be_{17}Hf_2$ consists of both forms or just one of them. The large energy difference obtained in our calculations indicates that one structure is much more likely than the other and the compound should consist exclusively of the Th_2Zr_{17} prototype.

One factor that might be of importance in calculations involving heavy elements is spin-orbit effects. In contrast to collinear spin calculations, a full consideration of the spin-orbit coupling of the local spins and the crystal structure requires non-collinear calculations which may reduce the symmetry of the system. These effects are not currently suitable for application in the high-throughput framework due to the excessive computational resources they demand. We carried out calculations to check the effect of spin-orbit interactions on ground states reported above for some of the binary systems of the heavier elements. These systems included examples of all the relevant transition metal crystal structure combinations: hcp–bcc (Hf–W), hcp–hcp (Hf–Os), hcp–fcc (Hf–Ir and Hf–Pt) and hcp–rhl (Hf–Hg). We also checked a few structures in the Hf–Tl system, where the new ground state predicted above is marginally stable, with a very small formation enthalpy of −2 meV atom^{-1}.

It is found that, although spin-orbit interactions can significantly affect the energies of specific structures, they do not change the relative stability of different structures and therefore do not qualitatively alter the convex hulls of these binary systems. The formation enthalpy of hcp–Hf is reduced from −9.952 eV atom^{-1} in the calculation neglecting spin-orbit to −10.657 eV atom^{-1} including spin-orbit. This difference of 705 meV atom^{-1} is quite large compared to the formation enthalpies reported in the 3rd column of Table 1. However, the changes obtained in these formation enthalpies, relative to the pure elements tie-lines, are much smaller. In the Hf–W system, the formation enthalpy of the stable structure C15 changes from −171 meV atom^{-1} (see Table 1) to −164 meV atom^{-1}, and a gap of 10 meV atom^{-1} is preserved from the next most stable structure, C36.

Similar results are obtained in the other systems. In the Hf–Pt system, including spin-orbit, the prototypes TlI and B33 remain degenerate and the most stable, and a considerable gap is preserved to the less stable B2 structure. A small gap also remains between the stable $D0_{24}$ prototype and the slightly less stable $L1_2$. Similarly, the degeneracy of the stable $C11_b$ and $CuZr_2$ structures is preserved in the Hf–Hg system. In the Hf–Tl system the changes obtained are more pronounced due to the small formation enthalpy of hcp-Tl. It is reduced by 12% from −2.365 eV atom^{-1} without spin-orbit to −2.667 eV atom^{-1} including spin-orbit. The formation enthalpy of the new $Hf_2Tl^{\star}$ ground state is reduced to −22 meV atom^{-1}. The calculation of this structure, with spin-orbit effects, required a cpu time 59.2 times longer than the previous calculation. Similar time factors in the other examples render this type of calculation inapplicable to extensive structure screenings even with today's development of computing power. It is therefore significant to note that these effects do not change the stability landscape of binary systems in all the examples checked in this study.

In conclusion, a systematic and comprehensive ab initio study of phase stability is carried out for the hafnium intermetallic systems. The total energies of about 200 intermetallic compounds have been calculated for 44 hafnium–metal systems and some interesting deviations from published experimental data were found. In particular, the calculations predict the existence of stable compounds in six hafnium intermetallic systems previously believed to be phase-separating. On the Pettifor chemical scale, three of these are isolated phase-separating systems in a cluster of compound-forming ones, and the discrepancy is likely due to the lack of experimental data. Hence, these predictions nicely complement the trend indicated by the empirical scale. A few new compounds are predicted in binary systems of Hf and other metals, and some compounds reported in the literature are shown to be unstable at low temperatures.

A detailed understanding of Hf alloys is crucial for a better realization of its potential as an alloying agent in currently available applications and in developing new ones. The picture of Hf alloys that emerges from this study is quite different from that depicted by current experimental data. It should be emphasized that we consider the alloys to be in thermodynamical equilibrium, which can be difficult to reach at low temperatures due to slow kinetics. At higher temperatures, configurational disorder and vibrational entropic promotion might destabilize the predicted compounds. The theoretical predictions presented here should therefore motivate research for their experimental validation and provide useful guidance to future studies of these alloys.

Acknowledgements

We thank Wahyu Setyawan, Leeor Kronik, and Mike Mehl for fruitful discussions. The research was supported by ONR (Grants N00014-07-1-0878, N00014-07-1-1085, N00014-09-1-0921) and NSF (DMR-0639822, DMR-0650406). We thank the Teragrid Partnership (Texas advanced Computing Center, TACC, MCA-07S005) and the Fulton Supercomputing Laboratory at Brigham Young University for computational support. S.C. acknowledges support from the Feinberg Fellowship at the Weizmann Institute of Science.

References

[1] Curtarolo S, Morgan D, Ceder G. CALPHAD 2005;29:163.
[2] Curtarolo S, Morgan D, Persson K, Rodgers J, Ceder G. Phys Rev Lett 2003;91(September):135503.
[3] Fischer CC, Tibbetts KJ, Morgan D, Ceder G. Nat Mater 2006;5:641.
[4] Jóhannesson GH, Bligaard T, Ruban AV, Skriver HL, Jacobsen KW, Nørskov JK. Phys Rev Lett 2002;88:255506.
[5] Lewis GJ, Sachtler JWA, Low JJ, Lesch DA, Faheem SA, Dosek PM, et al. J Alloys Compd 2007;355:446–7.
[6] Ortiz C, Eriksson O, Klintenberg M. Comput Mater Sci 2009;44:1042.
[7] Ozoliņš V, Majzoub EH, Wolverton C. Phys Rev Lett 2008;100:135501.
[8] Stucke DP, Crespi VH. Nano Lett 2003;3:1183.
[9] Cramer SD, Covino BS, editors. ASM handbook, 10th ed., vol. 13B. Metals Park (OH): ASM International; 2005.
[10] Wallenius J, Westlen D. Ann Nucl Energy 2008;35:60.
[11] Nielsen RH. Ullman's encyclopedia of industrial chemistry, vol. A12. Weinheim: VCH Verlagsgesellschaft; 1989. p. 559–69.
[12] Davidson JA. US Patent 5954724, September 21, 1999.
[13] Meng XL, Fu YD, Cai W, Li QF, Zhao LC. Phil Mag Lett 2009;89:431.
[14] Fernandes MT. Aluminum–magnesium–scandium alloys with hafnium. WO/2001/012868. World Intellectual Property Organization; 2001.
[15] Baudry A, Boyer P, Ferreira LP, Harris SW, Miraglia S, Pontonnier L. J Phys Condens Matter 1992;4:5025.
[16] Callegari A, Jamison P, Carrier E, Zafar S, Gusev E, Narayanan V, et al. Interface engineering for enhanced electron mobilities in W/HfO2 gate stacks. In: Electron devices meeting, IEDM technical digest. IEEE International, December 2004. Piscataway (NJ): IEEE; 2004. p. 825–8.
[17] Pignedoli CA, Curioni A, Andreoni W. Phys Rev Lett 2007;98:037602.
[18] Zhang JL, Evetts JE. J Mater Sci 1994;29:778.
[19] Belosević-Cavor J, Koteski V, Concas G, Cekic B, Novakovic N, Spano G. J Phys Chem Solids 2005;66:1815.
[20] Belosević-Cavor J, Koteski V, Novakovic N, Concas G, Congiu F, Spano G. Eur Phys J B 2006;50:425.
[21] Cekić B, Ivanović N, Koteski V, Koicki S, Manasijević M. J Phys Condens Matter 2004;16:3015.
[22] Chen XQ, Podloucky R. CALPHAD 2006;30:266.
[23] Chen XQ, Wolf W, Podloucky R, Rogl P. J Alloys Compd 2004;383:228.
[24] Chen XQ, Wolf W, Podloucky R, Rogl P. Phys Rev B 2005;71:174101.
[25] Ghosh G, van de Walle A, Asta M, Olson GB. CALPHAD 2002;26:491.
[26] Hao X, Wu Z, Xu Y, Zhou D, Liu X, Meng J. J Phys Condens Matter 2007;19:196212.
[27] Kong LT, Liu BX. J Phys Soc Jpn 2005;74:1766.
[28] Lalić MV, Cekić B, Popović ZS, Vukajlović FR. J Phys Condens Matter 1998;10:6285.
[29] Lalić MV, Popović ZS, Vukajlović RF. J Phys Condens Matter 1999;11:2513.
[30] Oh MW, Kima BS, Park SD, Weeb DM, Lee HW. Solid State Commun 2008;146:454.
[31] Ormeci A, Chu F, Wills JM, Mitchell TE, Albers RC, Thoma DJ, et al. Phys Rev B 1996;54:12753.
[32] Shein IR, Ivanovskii AL. J Phys Condens Matter 2008;20:415218.
[33] Zhang C, Zhang Z, Wang S, Li H, Dong J, Xing N, et al. J Alloys Compd 2008;448:53.
[34] Zhang X, Luo X, Han J, Li J, Han W. Comput Mater Sci 2008;44:411.
[35] Ghosh G. Acta Mater 2007;55:3347.
[36] Ghosh G, Asta M. Acta Mater 2005;53:3225.
[37] Ghosh G, van de Walle A, Asta M. Acta Mater 2008;56:3202.
[38] Hart GLW, Forcade RW. Phys Rev B 2008;77:224115.
[39] Villars P, Berndt M, Brandenburg K, Cenzual K, Daams J, Hulliger F, et al. J Alloys Compd 2004;367:293.
[40] Massalski TB, Okamoto H, Subramanian PR, Kacprzak L, editors. Binary alloy phase diagrams. Materials Park (OH): ASM International; 1990.
[41] Morgan D, Ceder G, Curtarolo S. Measur Sci Technol 2005;16:296.
[42] Curtarolo S, Setyawan W, Jahnatek M, Chepulskii RV, Hart GLW, Levy O, et al. AFLOW: software for high throughput calculation of material properties, <http://materials.duke.edu/aflow.html>; 2010.
[43] Levy O, Chepulskii RV, Hart GLW, Curtarolo S. J Am Chem Soc 2010;132:833.
[44] Kresse G, Hafner J. Phys Rev B 1993;47:558.
[45] Blochl PE. Phys Rev B 1994;50:17953.
[46] Perdew JP, Burke K, Ernzerhof M. Phys Rev Lett 1996;77:3865.

[47] Kolmogorov AN, Curtarolo S. Phys Rev B 2006;73:180501. R.
[48] Kolmogorov AN, Curtarolo S. Phys Rev B 2006;74:224507.
[49] Pettifor DG. Solid State Commun 1984;51:31.
[50] Pettifor DG. J Phys C Solid State Phys 1986;19(3):285–313.
[51] van de Walle A, Ceder G. Rev Mod Phys 2002;74:11.
[52] Wolverton C, Ozoliņš V. Phys Rev Lett 2001;86:5518.